Comparison of ^{87}Rb N-resonances for D_1 and D_2 transitions

Irina Novikova, David F. Phillips, Alexander S. Zibrov, and Ronald L. Walsworth

Harvard–Smithsonian Center for Astrophysics and Department of Physics, Harvard University, Cambridge, Massachusetts 02138

Aleksei V. Taichenachev and Valeriy I. Yudin

Institute of Laser Physics SB RAS and Novosibirsk State University, Novosibirsk, 630090, Russia

Received January 11, 2006; revised April 26, 2006; accepted May 8, 2006;
posted May 25, 2006 (Doc. ID 67202); published July 10, 2006

We report an experimental comparison of three-photon-absorption resonances (N-resonances) for the D_1 and D_2 optical transitions of thermal ^{87}Rb vapor. We find that the D_2 N-resonance has better contrast, a broader linewidth, and a more symmetric line shape than the D_1 N-resonance. Taken together, these factors imply superior performance for frequency standards operating on alkali D_2 N-resonances, in contrast with coherent population trapping resonances, for which the D_2 transition provides poorer frequency standard performance than the D_1 transition. © 2006 Optical Society of America

OCIS codes: 020.1670, 020.1670, 020.3690.

Recently, we demonstrated that three-photon-absorption resonances (N-resonances[1–3]) are a promising alternative to coherent population trapping (CPT) resonances[4–8] for small atomic frequency standards using thermal alkali vapor. Attractive features of N-resonances for atomic frequency standards include high resonance contrast, leading-order light-shift cancellation, and less sensitivity than CPT resonances to high buffer gas pressures,[2,3] which may provide improved short- and medium-term frequency stability compared with that of miniature CPT clocks. Previous work provided a comparative analysis of N- and CPT resonances[2] and demonstrated good short-term frequency stability for a bench-top ^{87}Rb N-resonance clock.[3]

In this Letter, we report an experimental comparison of N-resonances for the ^{87}Rb D_1 ($5^2S_{1/2} \rightarrow 5^2P_{1/2}$, $\lambda = 795$ nm) and D_2 ($5^2S_{1/2} \rightarrow 5^2P_{3/2}$, $\lambda = 780$ nm) optical transitions. We find similar N-resonance quality factors for the D_1 and D_2 transitions but a significantly more symmetric line shape for the D_2 transition, which together imply superior performance for a frequency standard using the D_2 N-resonance. Previous work has shown that the quality factor of alkali CPT resonances is about an order of magnitude worse for D_2 operation than for D_1.[9,10] Thus, as current miniature frequency standards rely on VCSELs that are readily available for the D_2 transitions of Rb and Cs but more difficult to acquire for the D_1 transitions, the results reported here provide an additional practical advantage for the N-resonance.

An N-resonance is a three-photon, two-optical-field absorptive resonance [Fig. 1(a)]. A probe field, Ω_P, resonant with the transition between the higher-energy hyperfine level of the ground electronic state and an electronically excited state, optically pumps the atoms into the lower hyperfine level, leading to increased transmission of the probe field through the medium. A drive field, Ω_D, is detuned from the probe field by the atomic hyperfine frequency, ν_0. Together, Ω_P and Ω_D create a two-photon Raman resonance that drives atoms coherently from the lower to the upper hyperfine level, thereby inducing increased absorption of the probe field Ω_P in a narrow resonance with linewidth, $\Delta\nu$, set by ground-state hyperfine decoherence.

Better performance for N-resonances than CPT resonances on the D_2 transition is expected due to the difference between the resonance mechanisms. The CPT transmission maximum appears as a result

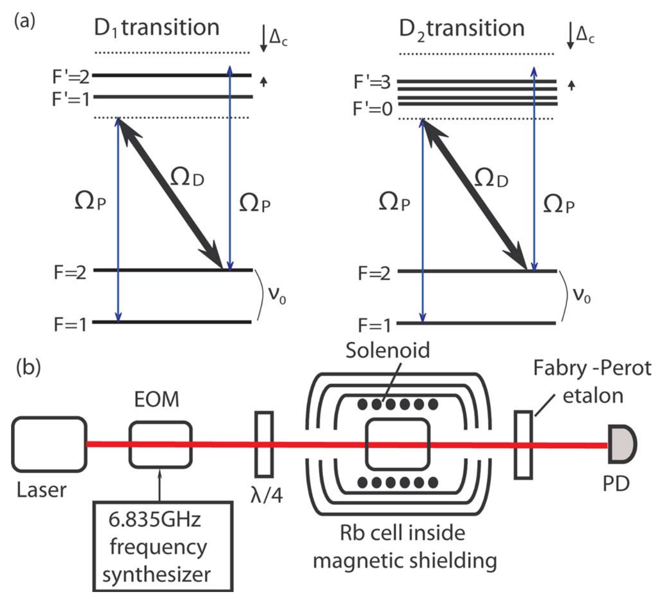

Fig. 1. (Color online) (a) N-resonance interaction scheme for the D_1 and D_2 transitions of ^{87}Rb. Ω_P and Ω_D are the probe and drive optical fields, respectively, that create and interrogate the N-resonance; ν_0 is the splitting of ground-state hyperfine levels $F=1$ and $F=2$; and Δ_c is the one-photon detuning of the probe field from resonance between the $F=2$ ground state and the excited state. (b) Schematic of the experimental setup. The optical fields Ω_P and Ω_D are derived from an external cavity diode laser, whose output is phase modulated by an electro-optic modulator (EOM) and circularly polarized by a quarter-wave plate ($\lambda/4$). The transmitted probe field is detected by a photodetector (PD).

0146-9592/06/152353-3/$15.00

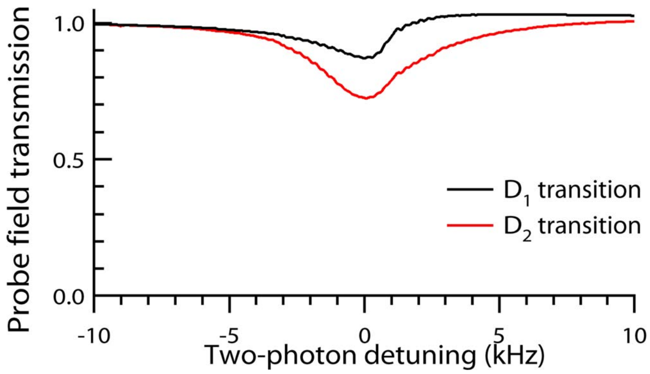

Fig. 2. (Color online) Example ^{87}Rb N-resonances observed for the D_1 and D_2 optical transitions. The laser power is $260\,\mu$W, corresponding to an intensity of $50\,\mathrm{mW/cm}^2$. The probe transmission is normalized to unity away from two-photon resonance.

of optical pumping of atoms into a noninteracting coherent superposition of two ground-state hyperfine levels (a dark state). However, a pure dark state exists only for the D_1 transition, thus the amplitude and contrast of CPT resonances are much higher for D_1 operation than for D_2.[9] For N-resonances, the three-photon absorptive process does not require a dark state, with no resultant advantage of D_1 over D_2. Furthermore, for circularly polarized light (commonly used in optically pumped atomic clocks) resonant with the D_1 transition, some atoms become trapped in the Zeeman state with maximum angular momentum—an end state ($F=2$, $m_F=\pm 2$ for ^{87}Rb)—which limits resonance amplitude and contrast on the ground-state $\Delta m_F=0$ hyperfine clock transition. However, for D_2 operation, the end state is coupled to the excited state through the cycling transition $F=2\rightarrow F'=3$. In the presence of strong collisional mixing in the excited state (induced by alkali–buffer gas collisions), the cycling transition suppresses optical pumping of atoms into the end state. Thus we expect higher resonance contrast for N-resonances operating on the D_2 transition.

Figure 1(b) shows a schematic of our N-resonance apparatus, which is similar to one used previously.[2,3] We used a Pyrex cell of 7 cm length and 2.5 cm diameter containing isotopically enriched ^{87}Rb and 100 Torr of Ne buffer gas (which induced excited-state collisional broadening of ≈ 2 GHz). We operated the system under conditions identified in our previous work to give good frequency standard performance. We set the laser detuning Δ_c and the electro-optic modulator modulation index to match the conditions for leading-order light-shift cancellation[3]: for D_1, $\Delta_c \approx +700$ MHz from the $F=2\rightarrow F'=2$ transition; for D_2, $\Delta_c \approx +500$ MHz from the $F=2\rightarrow F'=3$ transition; in both cases the modulation index is ≈ 0.8, corresponding to a probe/drive intensity ratio of about 19%.

Figure 2 shows examples of measured D_1 and D_2 N-resonances under identical conditions, with the probe field transmission normalized to unity away from two-photon resonance. Asymmetry in N-resonance line shapes is expected from interference of optical pumping in the real and dressed bases, due to the use of a far-detuned Raman transition.[11] Figure 3 shows the measured dependence on laser intensity of the N-resonance contrast, linewidth, and quality factor. We define resonance contrast as $C=1-T_{\min}/T_0$, where $T_{\min}$ and T_0 are the transmitted probe field intensities on two-photon resonance and away from resonance, respectively. The linewidth, $\Delta\nu$, is the measured full width at half-maximum, and the resonance quality factor is $q=C/\Delta\nu$. (The shot-noise limit to atomic clock frequency stability is inversely proportional to the quality factor; i.e., larger q corresponds to better frequency stability.[4]) As seen in Figs. 2 and 3, the typical measured N-resonance contrast is significantly larger for D_2 operation than for the D_1 transition, whereas the linewidth is broader for D_2 than for D_1. The differences in contrast and linewidth largely offset each other, such that the N-resonance quality factor is roughly comparable for the D_1 and D_2 transitions over a wide range of operating conditions. Note that in alkali vapor CPT resonances, the quality factor for the D_2 transition has been measured to be about an order of magnitude smaller than for the D_1 transition.[9,10]

Optically probed atomic frequency standards commonly employ slow modulation of the microwave drive and associated phase-sensitive detection as

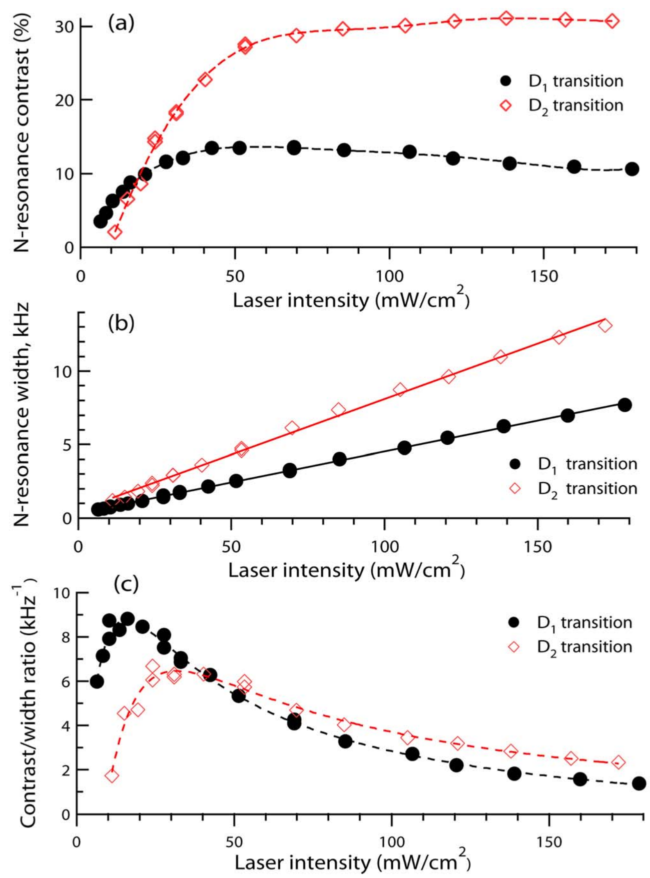

Fig. 3. (Color online) N-resonance (a) contrast C, (b) linewidth $\Delta\nu$, and (c) quality factor $q=C/\Delta\nu$, as a function of total input laser intensity, measured on the ^{87}Rb D_1 and D_2 transitions. The dashed curves are to guide the eye.

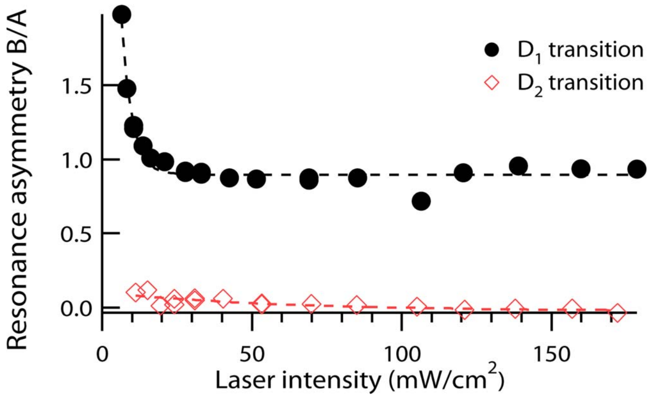

Fig. 4. (Color online) N-resonance asymmetry, B/A, as a function of laser intensity, determined from fits of a combination of symmetric and antisymmetric Lorentzian functions to measured N-resonance lineshapes; for D_1 and D_2 transitions. The dashed lines are to guide the eye.

part of the crystal oscillator lock-loop. Hence an asymmetric atomic resonance line shape can induce systematic frequency shifts proportional to the modulation parameters.[12] As seen in Fig. 2, ^{87}Rb N-resonances are significantly more symmetric for the D_2 transition than for D_1, which gives an important advantage for D_2 N-resonance operation. The asymmetry of the D_1 and D_2 N-resonance line shapes can be quantified by describing each measured N-resonance as a combination of symmetric and antisymmetric Lorentzian functions:

$$T = T_0 - \frac{(A\Delta\nu/2) + B\delta}{(\Delta\nu^2/4) + \delta^2}, \qquad (1)$$

where T is the measured probe field transmission as a function of two-photon Raman detuning, δ; and A, B, and $\Delta\nu$ are fit parameters that represent the amplitudes of the symmetric and antisymmetric Lorentzian components and the resonance linewidth. Figure 4 shows the ratio of antisymmetric and symmetric components, B/A, determined from our N-resonance line-shape measurements, as a function of laser intensity, indicating that the D_1 N-resonance is typically more than an order of magnitude more asymmetric than the D_2 N-resonance.

The greater asymmetry of the D_1 N-resonance line shape is expected from optical pumping into the dark state being more efficient on the Rb D_1 transition.[9] We find good quantitative agreement between the measured D_1 N-resonance asymmetry ($B/A \approx 1$) and predictions of a previous theoretical model.[11] We expect that similar agreement between experiment and theory for the D_2 N-resonance asymmetry will require inclusion in models of effects such as radiation trapping, propagation through a finite sample, and effects associated with nonresonant fields typically produced by a modulated laser. Such modeling is in progress.

In conclusion, N-resonances are three-photon-absorption resonances that are a promising alternative to CPT resonances for small atomic frequency standards using alkali atoms. Here, we report an experimental comparison of the D_1 and D_2 N-resonances in thermal ^{87}Rb vapor. We find that the D_2 N-resonance has better contrast but a broader linewidth than the D_1 N-resonance, such that the N-resonance quality factor is comparable for the D_1 and D_2 transitions. This result implies a similar shot-noise limit to N-resonance frequency standard performance on the D_1 and D_2 transitions, in stark contrast with CPT resonances, for which the quality factor is about an order of magnitude worse for the D_2 transition than for D_1. In addition, we find that the D_2 N-resonance line shape is significantly more symmetric than the D_1 line shape, indicating that a D_2 N-resonance frequency standard will have reduced sensitivity to certain modulation-induced systematic frequency shifts. Thus, unlike for CPT resonances, commercially available diode lasers for the D_2 lines of Rb and Cs can likely be used without compromising the performance of an N-resonance frequency standard.

We thank J. Vanier, C. Hancox, and M. Crescimanno for useful discussions. This work was supported by the Office of Naval Research, the Defense Advanced Research Projects Agency, the Institute for Theoretical Atomic, Molecular and Optical Physics, the Smithsonian, and RFBR (grants 05-02-17086, 05-08-01389, and 04-02-16488). I. Novikova's e-mail address is inovikova@cfa.harvard.edu.

References

1. A. S. Zibrov, C. Y. Ye, Y. V. Rostovtsev, A. B. Matsko, and M. O. Scully, Phys. Rev. A **65**, 043817 (2002).
2. S. Zibrov, I. Novikova, D. F. Phillips, A. V. Taichenachev, V. I. Yudin, R. L. Walsworth, and A. S. Zibrov, Phys. Rev. A **72**, 011801(R) (2005).
3. I. Novikova, D. F. Phillips, A. S. Zibrov, R. L. Walsworth, A. V. Taichenachev, and V. I. Yudin, Opt. Lett. **31**, 622 (2006).
4. J. Vanier, Appl. Phys. B **81**, 421 (2005).
5. S. Knappe, P. D. D. Schwindt, V. Shah, L. Hollberg, J. Kitching, L. Liew, and J. Moreland, Opt. Express **13**, 1249 (2005).
6. P. D. D. Schwindt, S. Knappe, V. Shah, L. Hollberg, J. Kitching, L. Liew, and J. Moreland, Appl. Phys. Lett. **85**, 6409 (2004).
7. A. B. Matsko, D. Strekalov, and L. Maleki, Opt. Commun. **247**, 141 (2005).
8. M. Merimaa, T. Lindwall, I. Tittonen, and E. Ikonen, J. Opt. Soc. Am. B **20**, 273 (2003).
9. M. Stahler, R. Wynands, S. Knappe, J. Kitching, L. Hollberg, A. Taichenachev, and V. Yudin, Opt. Lett. **27**, 1472 (2002).
10. R. Lutwak, D. Emmons, T. English, W. Riley, A. Duwel, M. Varghese, D. K. Serkland, and G. M. Peake, in *Proceedings of the 35th Annual Precise Time and Time Interval (PTTI) Systems and Applications Meeting* (U.S. Naval Observatory, 2003), p. 467.
11. A. V. Taichenachev, V. I. Yudin, R. Wynands, M. Stahler, J. Kitching, and L. Hollberg, Phys. Rev. A **67**, 033810 (2003).
12. D. F. Phillips, I. Novikova, C. Y.-T. Wang, M. Crescimanno, and R. L. Walsworth, J. Opt. Soc. Am. B **22**, 305 (2005).